Three-Dimensional Reciprocal Form Factors and Momentum Densities of Electrons from Compton Experiments

I. Symmetry-Adapted Series Expansion of the Electron Momentum Density

Eberhard Heuser-Hofmann and Wolf Weyrich
Fakultät für Chemie, Universität Konstanz

Z. Naturforsch. **40 a,** 99–111 (1985); received December 2, 1984

Dedicated to Prof. Dr. Alarich Weiss on the Occasion of his 60th Birthday

All methods of reconstruction of the electron momentum density from Compton scattering data are based on a series expansion of this density in terms of symmetry-adapted surface spherical harmonics (polyhedral harmonics). Owing to the improvements of γ-ray and X-ray Compton spectrometers during the last few years, measurements of Compton spectra of single crystals in a shorter time and with higher angular resolution have become feasible. Therefore, in addition to the current studies, an increased number of investigations of a greater variety of crystals with large sets of directional data will soon be performed. This work is at first concerned with the accurate and efficient computation of associated Legendre functions of the first kind, P_l^m, with high l and m and for the whole range of their real argument, which are needed for the description of data with high angular resolution. We further show that electron momentum densities obey Laue-class symmetries in the case of crystals and point-group symmetries with an inversion centre in general, in absence of external magnetic fields. All necessary information about the polyhedral harmonics belonging to the totally symmetric representations of these point groups is given, with particular emphasis on the group O_h for which the hexoctahedral harmonics with $l \leqq 20$ are displayed graphically. In addition, the locations of the extrema on the unit sphere are tabulated.

I. Introduction

Compton scattering of X-ray and γ-ray photons has proved to be a very sensitive and useful tool for the investigation of valence electron structure and chemical bonding in matter (for more comprehensive presentations see, e.g. [1–4]). From the Compton band in the spectra of such experiments, Compton profiles

$$J(p_z) = \int\int \hat{\varrho}(\boldsymbol{p})\, \mathrm{d}p_x\, \mathrm{d}p_y \qquad (1)$$

as projections of the three-dimensional electron momentum distribution (momentum density) $\hat{\varrho}(\boldsymbol{p})$ on the scattering vector $\boldsymbol{k} = \boldsymbol{k}_2 - \boldsymbol{k}_1$ can be extracted. The momentum coordinate p_z in (1) is oriented in the direction of $\boldsymbol{k}$, while p_x and p_y are perpendicular to it, and $\boldsymbol{k}_1$, $\boldsymbol{k}_2$ are the wave vectors of the incoming and outgoing photons, respectively.

If the sample is isotropic (gases, liquids, glasses, powders etc.), the momentum density seen by the experiment is spherically symmetrical, and hence one obtains a directionally independent Compton profile,

$$J(p_z) = \int\int \hat{\varrho}(p)\, \mathrm{d}p_x\, \mathrm{d}p_y\,. \qquad (2)$$

It can be rewritten in spherical momentum coordinates as

$$J(q) = 2\pi \int_{|q|}^{\infty} \hat{\varrho}(p)\, p\, \mathrm{d}p\,. \qquad (3)$$

By differentiation of this equation one can calculate the spherically symmetrical momentum density

$$\hat{\varrho}(p) = -\frac{1}{2\pi p}\,\frac{\mathrm{d}J(p)}{\mathrm{d}p}\,, \qquad (4)$$

a relationship which was already known to the pioneers in the field [5] and which restricts the spherically symmetrical $J(q)$ to have a single maximum at $q = 0$ owing to the positive-definiteness of $\hat{\varrho}(p)$.

If, on the other hand, the specimen is a single crystal, the orientation of the line of projection can be varied with respect to the crystal coordinate

---

Reprint requests to Prof. Dr.-Ing. W. Weyrich, Fakultät für Chemie, Universität Konstanz, Postfach 55 60, D-7750 Konstanz.

0340-4811 / 85 / 0200-0099 $ 01.30/0. – Please order a reprint rather than making your own copy.

system, and thus the three-dimensional Compton profile function

$$J(\boldsymbol{q}) = \int\int\int \hat{\varrho}(\boldsymbol{p})\, \delta(\boldsymbol{p}\cdot\boldsymbol{q} - q^2)\, \mathrm{d}\boldsymbol{p} \qquad (5)$$

can be sampled along radial lines $\boldsymbol{q} = (q, \theta_q, \varphi_q)$ with constant orientation θ_q, φ_q and variable radial distance q in momentum space. With the choice of $\boldsymbol{q}$ in (5) instead of p_z in (1) we have passed from the $\boldsymbol{k}$ coordinate system to the crystal coordinate system.

The Compton profile function $J(\boldsymbol{q})$ suffices in principle to describe the electron momentum properties in three dimensions. The directional dependence of the kinetic energy T_e of the electrons, for example, can easily be evaluated from $J(\boldsymbol{q})$, and the tensorial property of T_e [6–8] imposes not only experimentally interesting general restrictions on $J(\boldsymbol{q})$ [8] in addition to some special cases [9].

Nevertheless, it is desirable for a more direct interpretation and understanding to obtain the electron momentum distribution $\hat{\varrho}(\boldsymbol{p})$ itself. In order to achieve this, the integral equation (5) has to be solved. The first solution to this problem is due to Mijnarends [10–12] and has been applied to positron annihilation data of some metals [13–15] as well as to Compton profiles of diamond and silicon [16, 17]. An improvement of the method of Mijnarends has been suggested by Majumdar [18]. A second approach based on the differentiation and Fourier transformation of Compton profiles has been introduced and tested by Mueller [19, 20] on silicon data measured by Reed [21].

Our method [22, 2, 23–26] is closely related to the latter approach, but avoids the drawback of differentiation of experimental data and does not restrict itself to the anisotropic part. It rather uses the full Fourier transform of $\hat{\varrho}(\boldsymbol{p})$, the reciprocal form factor $B(\boldsymbol{r})$, and thus allows at the same time an analysis of the momentum space information in its position space representation.

The aim of the present series of papers is to summarise and to extend our work [2, 25, 26] on that method. It will, at the same time, form the basis for future three-dimensional studies which have become feasible and desirable following experimental improvements both with γ-rays (^{241}Am [2, 25, 27–32], ^{198}Au [33, 34]) and X-rays [35].

The present Part I deals with the series expansion of $\hat{\varrho}(\boldsymbol{p})$ as the common basis of all the above mentioned reconstruction methods followed by a presentation and discussion of the surface spherical harmonics which are symmetry-adapted to the Laue class O_h (hexoctahedral harmonics).

The forthcoming Part II will compare the reconstruction methods, specialise on the method via the reciprocal form factor with its mathematical details and analyse the propagation of experimental errors and the question of the best choice of directions θ_q, φ_q in the experiment.

Part III will be devoted to the three-dimensional momentum density and the reciprocal form factor of crystalline lithium fluoride.

II. The Single-Centre Expansion

The common basis of all methods used so far for the solution of the integral equation (5) is the expansion of the momentum density $\hat{\varrho}(\boldsymbol{p})$ into a series of suitable functions. Since $\hat{\varrho}(\boldsymbol{p})$ is single-centred with a dominant spherically symmetrical part, the natural choice is the subdivision of momentum space into radial shells in a spherical coordinate system and the description of $\hat{\varrho}(\boldsymbol{p})$ on each shell by a series of angular functions $X_L(\theta_p, \varphi_p)$ with weights $\hat{\varrho}_L(p)$,

$$\hat{\varrho}(\boldsymbol{p}) = \sum_L \hat{\varrho}_L(p) \cdot X_L(\theta_p, \varphi_p)\,. \qquad (6)$$

Ideally the X_L should form a complete orthogonal basis set on the surface of the unit sphere, a condition which is fulfilled both by the complex

$$Y_l^m(\theta, \varphi) = \left[\frac{(2l+1)(l-m)!}{(l+m)!}\right]^{1/2} \cdot P_l^m(\cos\theta)\, e^{im\varphi} \qquad (7)$$

and the real

$$S_l^m(\theta, \varphi) = \left[\frac{2(2l+1)(l-|m|)!}{(1+\delta_{m,0})(l+|m|)!}\right]^{1/2} P_l^{|m|}(\cos\theta) \cdot \begin{cases} \cos(|m|\varphi) & \text{if} \quad m \geqq 0 \\ \sin(|m|\varphi) & \text{if} \quad m < 0 \end{cases} \qquad (8)$$

surface spherical harmonics (Kugelflächenfunktionen*) with $l = 0, 1, 2, \ldots$ and $-l \leqq m \leqq l$. In quantum chemistry the former are often called "spherical harmonics" (although this name covers the whole

---

* The nomenclature is so inconsistent and hence conceptually misleading in literature that for our field we propose a standardised bilingual terminology which deviates as little as possible from traditional mathematical usage.

family of functions Y which are solutions to the angular part of the Laplace equation in spherical coordinates,

$$\Delta_{\theta,\varphi}\, Y = 0\,, \tag{9}$$

or even the family of functions V which are homogeneous in x, y, z and satisfy the complete Laplace equation,

$$\Delta V = 0\,, \tag{10}$$

cf. Hobson [36], p. 119; "Kugelfunktionen"), the latter "surface harmonics" as the second possibility to abbreviate the complete name. Note that we normalise, in agreement with Mijnarends [10–12], all surface spherical harmonics to 4π in order to facilitate the analysis of the magnitude of the $\hat{\varrho}_L(p)$ in relation to $\hat{\varrho}(\boldsymbol{p})$ itself.

III. Computation of the Associated Legendre Functions

The P_l^m are the associated Legendre functions of the first kind (zugeordnete Legendresche Kugelfunktionen erster Art) defined via the Legendre polynomials $P_l(x)$ by

$$P_l^m(x) = (-1)^m (1-x^2)^{m/2} \frac{\mathrm{d}^m}{\mathrm{d}x^m} P_l(x) \tag{11}$$

$$= \frac{(-1)^{m+l}}{2^l\, l!} (1-x^2)^{m/2} \frac{\mathrm{d}^{l+m}}{\mathrm{d}x^{l+m}} (1-x^2)^l \tag{12}$$

for real $-1 \leqq x \leqq 1$, the phase factor chosen following Hobson [36], Magnus et al. [37], Abramowitz and Stegun [38], and Gradshteyn and Ryzhik [39]*.

For negative m, (11) implies an m-fold integration, while (12) treats negative m by a reduction of the number of differentiations. Between positive and negative m the relations

$$P_l^{-m}(x) = (-1)^m \frac{(l-m)!}{(l+m)!} P_l^m(x) \tag{13}$$

and hence

$$Y_l^{-m} = (-1)^m\, Y_l^{m*} \tag{14}$$

exist.

The associated Legendre functions P_l^m can be represented as hypergeometric functions ${}_2F_1$ in 36 different ways [37], a very popular one of which is

$$P_l^m(x) = \frac{1}{\Gamma(1-m)} \left(\frac{1+x}{1-x}\right)^{m/2} \cdot {}_2F_1\left(-l, l+1; 1-m; \frac{1-x}{2}\right) \tag{15}$$

(cf. Ref. [38], (8.1.2) and (15.4.17)).

By use of (13) and the relation (see [37], p. 152)

$${}_2F_1(a, b; c; \zeta) = (1-\zeta)^{c-a-b}\, {}_2F_1(c-a, c-b; c; \zeta) \tag{16}$$

it can be rewritten as

$$P_l^m(x) = \left(-\frac{1}{2}\right)^m \frac{(l+m)!}{(l-m)!} \cdot \frac{1}{m!} \cdot (1-x^2)^{m/2} \cdot {}_2F_1\left(m+l+1, m-l; 1+m; \frac{1-x}{2}\right). \tag{17}$$

Mijnarends [10–12] and Hansen [23] have employed this equation for the computation of $P_l^m(x)$, Mijnarends with omission of the factor $(-1)^m$ because of even m.

There further exist the recursion equations (see [37], p. 171)

$$(l-m+1)\, P_{l+1}^m(x) = (2l+1)\, x\, P_l^m(x) - (l+m)\, P_{l-1}^m(x) \tag{18}$$

and

$$(1-x^2)^{1/2} P_l^{m+1}(x) = (l-m)\, x\, P_l^m(x) - (l+m)\, P_{l-1}^m(x) \tag{19}$$

which, starting from $P_0^0 = 1$, $P_1^0 = x$, are numerically reasonably stable for not too high l and m and have been used by us earlier [25]; the undetermined 0/0 of (19) for $P_l^{m+1}(x)$ at $x = \pm 1$ can be overcome by setting $x = \pm(1-\varepsilon)$.

---

* "There is considerable variation in the notation employed by writers on the subject with reference to the associated Legendre's functions." (Hobson [36].) This is still true for the phase factor. Rose [40], Messiah [41], Spain and Smith [42], Kara and Kurki-Suonio [43] as well as Korn and Korn [44] omit the factor $(-1)^m$ in (11); only [40–43] introduce it in (7) instead, while neither of [43, 44] compensates it in (8). Sneddon [45] differs in his P_l^m by another factor of i^m and additionally uses Ferrer's function T_l^m which is identical to the P_l^m of Rose etc. The concordance equations

$$P_l^m = (-1)^m\, T_l^m = (-1)^m\, (P_l^m)_{[40-44]} = i^m\, (P_l^m)_{[45]}\,,$$
$$Y_l^m = (-1)^m\, (Y_l^m)_{[44]}\,,$$
$$S_l^m = (-1)^m\, (S_l^m)_{[43,\,44]}$$

hold. It would be very unfortunate if such a sign confusion would persist in our field, since tables of the $\hat{\varrho}_L(p)$ and $B_L(r)$ will be a useful and concise means of reporting experimental and theoretical three-dimensional data. Because of the phase factor question also special care is necessary when formulae for complex arguments z are to be used for real arguments x.

Not only the recursion formulae (18) and (19) tend to have numerical instabilities because of differences between almost equal numbers. Such differences occur in all algorithms known to us for the computation of the P_l^m. Written as an explicit hypergeometric series, the ${}_2F_1$ in (17) becomes*

$$
{}_2F_1\left(m+l+1, m-l; 1+m; \frac{1-x}{2}\right) \tag{20}
$$
$$
=1+\sum_{k=1}^{l-m}\left\{(-1)^k \prod_{j=1}^{k}\left[\frac{(m+l+j)(l-m-j+1)}{j(m+j)}\cdot\frac{1-x}{2}\right]\right\},
$$

i.e. a polynomial in $(1-x)/2$ of degree $l-m$ with alternating signs. The differentiations of (12) can be carried out in closed form and yield

$$
P_l^m(x)=\frac{(-1)^{l+m}}{2^l}(1-x^2)^{m/2} \tag{21}
$$
$$
\cdot\sum_{k=k_0}^{l}(-1)^k\frac{(2k)!}{k!(l-k);(2k-l-m)!}\cdot x^{2k-l-m}
$$

with $k_0=[(l+m+1)/2]$, i.e. again a polynomial of degree $l-m$ with alternating signs, but this time in x itself and with only even or odd powers.

The angular resolution of 3° FWHM in our Compton experiments, in combination with statistical precision based on typically $4\cdot 10^7$ photons per Compton profile enables us to analyse finer details of the momentum density $\hat{\varrho}(\boldsymbol{p})$ and the reciprocal form factor $B(\boldsymbol{r})$ [25, 26]. Such an improved experimental level naturally requires an increased effort, which has been cited in [4] as "a patient endeavour unlikely to be equalled", but which, we can say, is worthwhile and is certainly going to be the future standard. The description of high angular resolution data requires high l and m in the P_l^m and a large number of terms in (6). Hence it is important to care about numerical reliability and efficiency in the computation of the P_l^m.

For small pole distances θ, i.e. $x=\cos\theta$ close to $+1$, the argument $(1-x)/2$ of (17) and (20) is small, and the finite series converges rapidly. Hence numerically accurate results are obtained. With increasing pole distance θ, however, $(1-x)/2$ gets larger, and the series (which is, at the same time, a Taylor expansion around $\theta=0$) becomes numerically very ill-behaved for higher θ. At $\theta=\pi$, the series is even singular for complex arguments and indices z, λ, μ (cf. [38], (8.1.2)). It was this numerical instability which led us to deal with P_l^m in more detail. Since, at the same time, the polynomial in $(1-x)/2$ requires the computation of approximately twice as many terms (analytically the wrong powers of x cancel), we can only advise against this algorithm.

Our algorithm (21) with a polynomial in powers x^{2k-l-m} (cf. also [36], p. 95, (9) and [39], second part of (8.812), for alternative formulations) shows none of these drawbacks. It requires the minimum number of terms and is numerically stable over the whole range $1\geqq x\geqq -1$, $0\leqq\theta\leqq\pi$; only 7 (!) decimal digits are lost in the worst case of P_{20}^0 at the poles.

While there is no doubt that (21) is the most suitable algorithm for the calculation of a single $P_l^m(x)$, in (6) a whole series of $P_l^m(x)$ with the same argument x is required. In such a situation, recursion formulae of the type of (18) and (19) are more efficient, provided θ is not at or close to the poles, where the algorithm of (21) has to be taken.

IV. Symmetry Adaptation

Although the real surface spherical harmonics S_l^m provide a complete orthogonal basis set for the expansion in (6), it is desirable to introduce the symmetry of $\hat{\varrho}(\boldsymbol{p})$ in order also to ensure that the expansion has the right symmetry. In experimentally necessarily finite expansions, the introduction of symmetry reduces the number of independent terms L and hence the required number of sets of experimental data for a certain angular resolution.

Such symmetry adaptations have a long history, which we can only hope to sketch without even claiming to be representative. Our aim is to clarify the origin and the distinction between different types of symmetry adaptation.

On the one hand, we have the point-group symmetry. It was first considered in connection with solutions to the Laplace and the Helmholtz equation with polyhedral boundary conditions (Klein [46], Goursat [47], Pockels [48], Poole [49], Hodgkinson [50], Laporte [51]), in connection with the problem of term splitting when passing from spherical symmetry to another point symmetry (Bethe [52], see also the whole literature on ligand-field

---

* Note that the first part of Eq. (8.812) of [39] is in error by using $(l-m+j+1)$; cf. [36], p. 95, Eq. (11).

theory), and in connection with the rotational-vibrational spectrum of the methane molecule (Ehlert [53], Jahn [54, 55], Hecht [56], Moret-Bailly [57], Fox and Ozier [58]). Systematic group-theoretical studies for a larger number of point groups are due to Laporte [51], Meyer [59], Melvin [60], Altmann [61, 62], Döring [63], Bradley and Cracknell [64], and Kurki-Suonio et al. [65, 66, 43]. Owing to the long period over which the literature is spread, the focus of interest and the formalisms are very heterogeneous. The major differences are the inclusion of powers of the radial distance as the third dimension (solid spherical harmonics, "Kugelvolumenfunktionen" V) or exclusion (surface spherical harmonics, "Kugelflächenfunktionen" Y), cartesian coordinates (x, y, z für V, direction cosines x/r, y/r, z/r for Y) or polar coordinates, the group-theoretical method and normalisation factors. The nomenclature for the resulting symmetry-adapted surface spherical harmonics

$$X_L = \sum_{l,m} C_{lmL} S_l^m \tag{22}$$

is also very variable. "Symmetry-adapted functions" [60] is too general, and we therefore use the precise and pictorial name "polyhedral (surface spherical) harmonics" = "polyedrische Kugelflächenfunktionen" [49–51]. They *are* functions on the surface of the unit sphere and possess the symmetry of a polyhedron. The name of the polyhedron specific for a point group should be chosen according to the nomenclature for the 32 crystal classes in the "International Tables for Crystallography" ([67], p. 786, Tab. 10.6.1).

There is the space-group symmetry, on the other hand, which imposes additional boundary conditions by its translational operations. The adaptation of functions to the symmetry of a space group has been introduced in connection with the theoretical calculation of the electronic structure of solids (Wigner and Seitz [68], Bouckaert, Smoluchowski and Wigner [69]) and has been further developed by von der Lage and Bethe [70], Howard and Jones [71], Bell [72] and Altmann and co-workers [73–75]. A position-space function $f(\boldsymbol{r}, \boldsymbol{k})$ which fulfils the Bloch condition

$$f(\boldsymbol{r} + \boldsymbol{t}_{uvw}, \boldsymbol{k}) = f(\mathbf{r}, \boldsymbol{k}) \cdot \exp(i\boldsymbol{k} \cdot \boldsymbol{t}_{uvw}) \tag{23}$$

in a lattice of translation vectors $\boldsymbol{t}_{uvw}$ can be expanded in analogy to Eq. (6), but around a multitude of centres $\boldsymbol{t}_{uvw}$, in terms of

$$\Lambda_{\boldsymbol{k}L} = \sum_{uvw} \exp(i\boldsymbol{k}\boldsymbol{t}_{uvw}) \cdot {}^{uvw}X_L(\theta, \varphi) \, . \tag{24}$$

The symmetry-adapted, multicentred functions $\Lambda_{\boldsymbol{k}L}$ are called "lattice harmonics" ("Gitterkugelflächenfunktionen") following Bell [72], as clarified by Altmann and Cracknell [74]. If the space group is symmorphic, i.e. does not contain any screw axes or glide planes with their non-lattice translations, then the ${}^{uvw}X_L$ centred at the various $\boldsymbol{t}_{uvw}$ are the polyhedral harmonics X_L of the point group [74]. This fact has led to the confusion of using the name "lattice harmonics" for the X_L. In the case of asymmorphic space groups, one has to follow a more complicated procedure [75] based on a group-theoretical approach owing to Herring [76]. For a hexagonal close-packed lattice ($D_{6h}^4 = P6_3/mmc$), e.g., the resulting X_L are double-centred within the unit cell [75], i.e. they are not polyhedral harmonics.

Because of the peridocity of the electron position density $\varrho(\boldsymbol{r})$ in a crystal,

$$\varrho(\boldsymbol{r} + \boldsymbol{t}_{uvw}) = \varrho(\boldsymbol{r}) \, , \tag{25}$$

lattice harmonics with $\boldsymbol{k} = 0$ are the appropriate basis for as series expansion. This is the principle of the method owing to Atoji [77], which consists of a single-centre expansion of the right-hand side of (25) in a unit cell (or Wigner-Seitz cell) and of a repetition of it with the translational lattice $\boldsymbol{t}$ under fulfilment of the boundary condition of continuity at the cell surfaces. With more than one atom in the unit cell or Wigner-Seitz cell the single-centre expansion converges very slowly, and the cell boundary conditions are involved. Hence rapidly converging expansions around every atom have been introduced (Weiss et al. [78, 79], Dawson et al. [80–82], Kurki-Suonio et al. [83, 84, 65, 66, 43], Stewart [85–90] and Hirshfeld et al. [91–93]), now with the problem of overcompleteness of the basis sets and with similar solutions to it as in quantum chemistry (truncated series, analytical radial functions).

Such a problem does not occur in momentum space. The electron momentum density, $\hat{n}(\boldsymbol{p})$, in the repeated zone scheme of the reciprocal lattice,

$$\hat{n}(\boldsymbol{p}) \equiv \sum_{hkl} \hat{\varrho}(\boldsymbol{p} - \hat{\boldsymbol{t}}_{hkl}) \, , \tag{26}$$

can be expressed by a well converging series of lattice harmonics (cf. Part II), since the constituent momentum density, $\hat{\varrho}(\boldsymbol{p})$, is single-centred.

Table 1. The Laue classes and their polyhedral harmonics. The selection rules for the indices m of the S_l^m are taken from [43, 64, 66] and are based on z as the polar axis. The integer number k is $\geqq 0$, while the index l is non-negative and even in all cases because of the inversion centre.

Laue class (point group)	Polyhedron	Selection rule	
$C_i = \bar{1}$	pinacoidal	$m = \pm k$	
$C_{2h} = 2/m$	prismatic	$m = \pm 2k$ $m = k$ $m = (-1)^k \cdot k$	for $2 \parallel z$ for $2 \parallel y$ (crystallogr. setting) for $2 \parallel x$
$D_{2h} = mmm$	dipyramidal	$m = 2k$	
$C_{4h} = 4/m$	tetragonal-dipyramidal	$m = \pm 4k$	for $4 \parallel z$
$D_{4h} = 4/mmm$	ditetragonal-dipyramidal	$m = 4k$	for $4 \parallel z, m \perp z, m \perp x, m_{\text{diag.}}$
$C_{3i} = \bar{3}$	rhombohedral	$m = \pm 3k$	for $\bar{3} \parallel z$
$D_{3d} = \begin{cases} \bar{3}1m\,(m \perp y) \\ \bar{3}m1\,(m \perp x) \end{cases}$	(ditrigonal-)scalenohedral	$\begin{cases} m = 3k \\ m = (-1)^k \cdot 3k \end{cases}$	for $\bar{3} \parallel z, m \perp y$ for $\bar{3} \parallel z, m \perp x$
$C_{6h} = 6/m$	hexagonal-dipyramidal	$m = \pm 6k$	for $6 \parallel z$
$D_{6h} = 6/mmm$	dihexagonal-dipyramidal	$m = 6k$	for $6 \parallel z$
$T_h = m\bar{3}$	disdodecahedral	special linear combinations of S_l^m with either $m = 4k$ or $m = 4k + 2$ (see Ref. [64, 74], one-dimensional representation, symmetry A_g, for $l \leqq 12$)	
$O_h = m\bar{3}m$	hexoctahedral	special linear combinations of S_l^m with $m = 4k$ (see Ref. [98] for $l \leqq 30$, Ref. [97] for $l \leqq 100$)	

Because of the lack of translational symmetry in $\hat{\varrho}(\boldsymbol{p})$, the functions X_L in (6) have to be adapted to a pure point-group symmetry and are therefore polyhedral harmonics. (The use of the notion "lattice harmonics" for them is wrong, as explained above.) The momentum density $\hat{\varrho}(\boldsymbol{p})$ possesses inversion symmetry in systems which can be described by real position-space wave functions (Löwdin [94]). Pictorially, electrons follow their trajectories in both directions with equal probability as long as there is no magnetic field; only in a magnetic field there is one direction preferred according to Lenz's rule with a (very small) deviation of $\hat{\varrho}(\boldsymbol{p})$ from inversion symmetry [2]. Therefore the point groups which describe the symmetry of $\hat{\varrho}(\boldsymbol{p})$ must contain an inversion centre, and for experiments on single crystals the only possible point groups are the 11 Laue classes.

For the Laue classes C_i, C_{2h}, D_{2h}, C_{4h}, D_{4h}, $C_{3i} = S_6$, D_{3d}, C_{6h} and D_{6h}, the symmetry adaptation of the real surface spherical harmonics S_l^m yields index selection rules which are summarised by Bradley and Cracknell [64] and by Kurki-Suonio et al. [65, 66, 43] and which we have compiled in Table 1. Owing to the inversion centre, only even l are allowed; all other selection rules concern the index m (note its definition by (8)). In the notation of (22), the selection rules mean that for every L the sum consists of a single term with $C_{lmL} = 1$ with an allowed pair of values for the indices l, m; all other $C_{l'm'L}$ for that L are zero. The index L of the polyhedral harmonics X_L is then either represented by the pair l, m, leading to the notation X_l^m, or by l and the current number n of the allowed m with the notation $X_{l,n}$, or just by the current number L of the allowed pair l, m, i.e. X_L. The last two notations depend on the Laue class, and therefore the Schönflies or Hermann-Mauguin symbol should be attached wherever necessary for clarity. In the Laue class $C_{2h} = 2/m$, e.g., the equality $X_2^2 = X_{2,3}^{2/m} = X_4^{2/m}$ would hold for the fourth prismatic harmonic in all three settings.

Before we concentrate on the Laue classes T_h and O_h, also non-crystallographic point groups should be mentioned. They are collected with their selection rules in Table 2. They are needed for the series expansion of theoretical momentum densities of molecules (the "partial wave analysis" of Thakkar, Simas and Smith [95]), but also for the representation of experimental data of samples with macroscopically superimposed non-crystallographic (dis)order, such as the point group $D_{\infty h}$ for pyrolytic

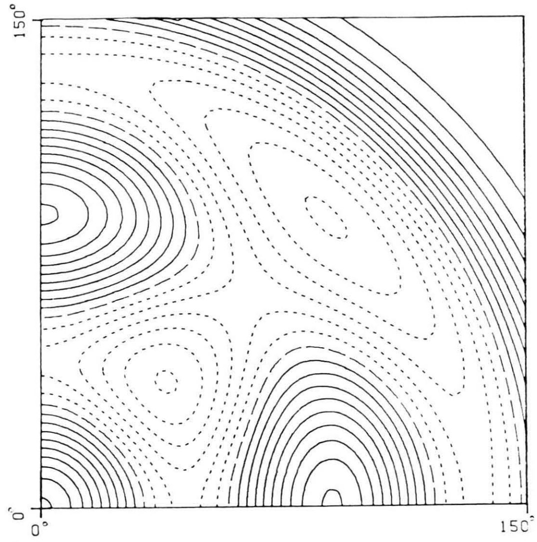

a)

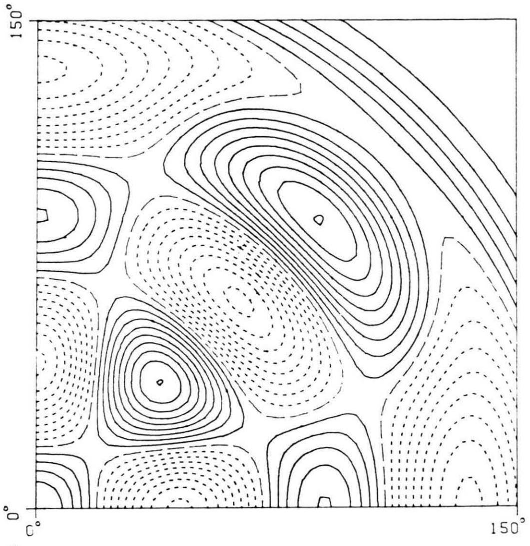

b)

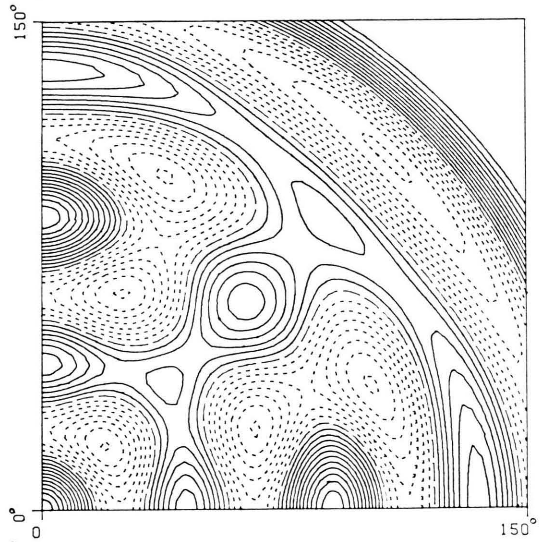

c)

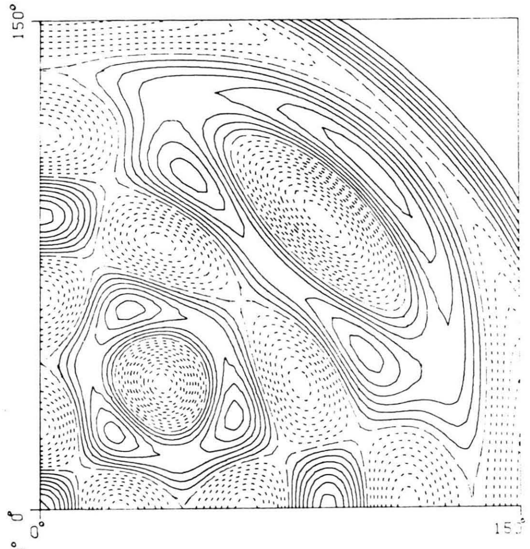

d)

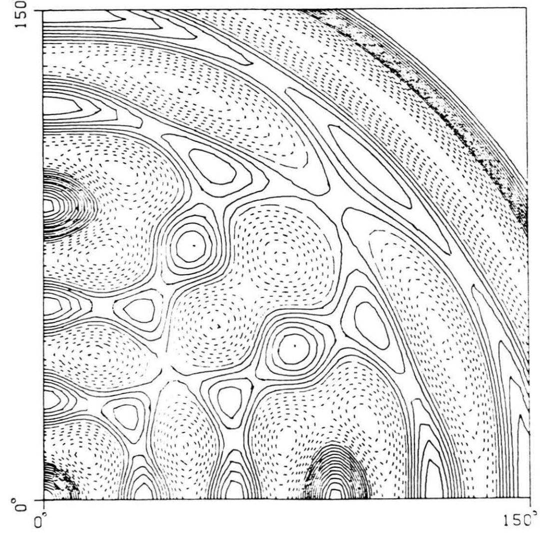

e)

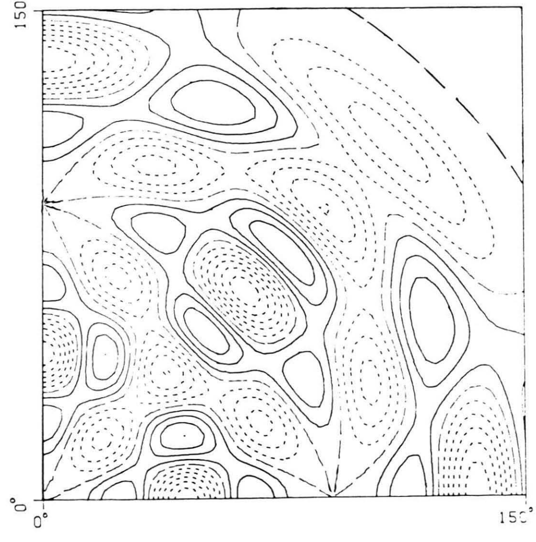

f)

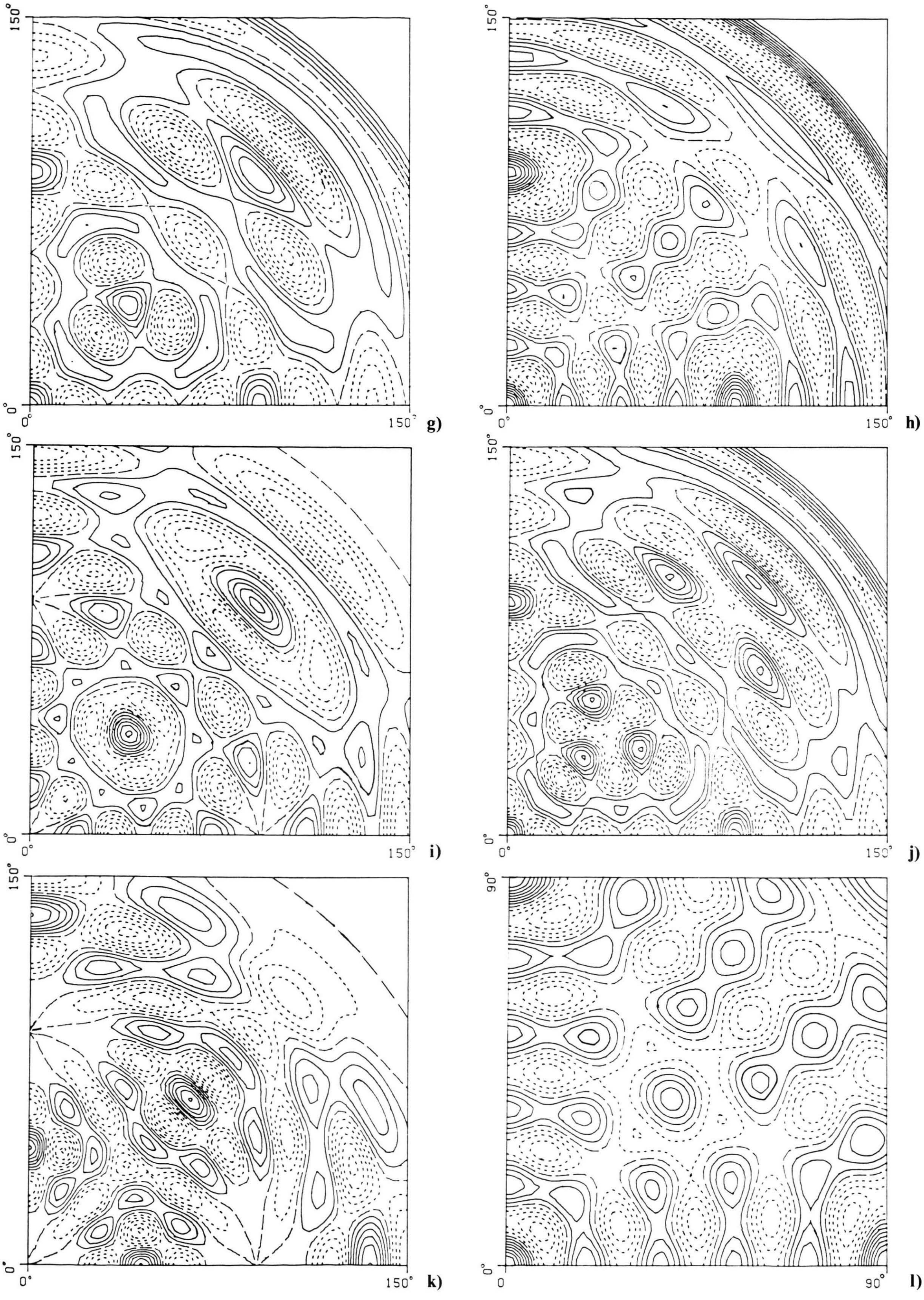
150°
0°
0°
150°
g)
150°
0°
0°
150°
h)
150°
0°
0°
150°
i)
150°
0°
0°
150°
j)
150°
0°
0°
150°
k)
90°
0°
0
90°
l)

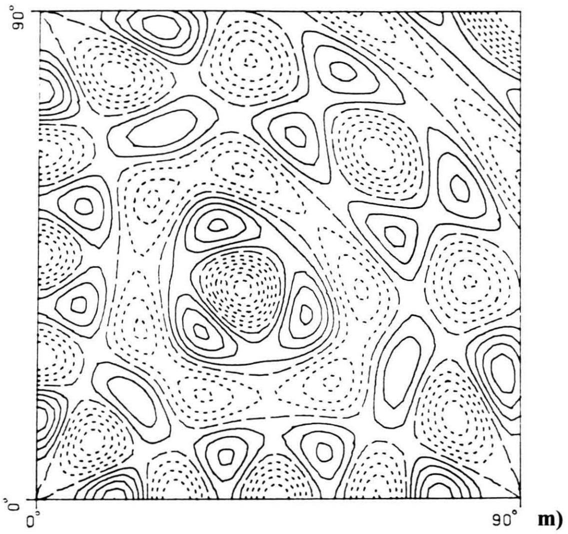

Fig. 1 a–m. Contour diagrams of the hexoctahedral harmonics $L = 2$ to $L = 14$ ($l = 4$ to $l = 20$) on the first azimuthal quadrant of the unit sphere. The radial coordinate is the pole distance θ with the range $0 \leqq \theta \leqq 180°$ for $L = 2$ to 12 and $0 \leqq \theta \leqq 127°$ for $L = 13$ and 14, the angular coordinate the azimuthal angle φ with the range $0° \leqq \varphi \leqq 90°$. Positive contours are full lines, negative contours are lines with short dashes, and the nodes are lines with long dashes. The contour distance is 0.25 for $L = 2$ to 6 and 0.5 for $L = 7$ to 14. Note that, owing to the mapping, only the symmetry around the polar [001]-direction is undistorted, and that the point of the $[00\bar{1}]$-direction forms a limiting circle.

Table 2. Some non-crystallographic molecular point groups and their polyhedral harmonics with index selection rules for the S_l^m. For the values of k and l see Table 1.

Point group	Polyhedron	Selection rule		
$C_{5i} = \bar{5}$	pentagonal-dipyramidal	$m = \pm 5k$	for $\bar{5} \parallel z$	
$D_{5d} = \begin{cases} \bar{5}\,1\,m\ (m \perp y) \\ \bar{5}\,m\,1\ (m \perp x) \end{cases}$	dipentagonal-dipyramidal	$m = 5k$ $m = (-1)^k \cdot 5k$	for $\bar{5} \parallel z,\ m \perp y$ for $\bar{5} \parallel z,\ m \perp x$	
$C_{ji} = \bar{j}$	j-gonal-dipyramidal	$m = \pm jk$	for $j \parallel z$	j odd
$D_{jd} = \begin{cases} \bar{j}\,1\,m\ (m \perp y) \\ \bar{j}\,m\,1\ (m \perp x) \end{cases}$	di-j-gonal-dipyramidal	$m = jk$ $m = (-1)^k \cdot jk$	for $j \parallel z,\ m \perp x$ for $j \parallel z,\ m \perp x$	
$C_{jh} = j/m$	j-gonal-dipyramidal	$m = \pm jk$	for $j \parallel z$	j even
$D_{jh} = j/mmm$	di-j-gonal-dipyramidal	$m = jk$	for $j \parallel z$	
$D_{\infty h} = \infty/mmm$	(di)cylindrical	$m = 0$	for $\infty \parallel z$	
$Y_h = 5\,3\,m$	icosahedral	special linear combinations of S_l^m with $m = 5k$ (see Ref. [51, 96, 43])		

graphite, or other partially ordered systems such as liquid crystals. For details of the icosahedral harmonics the reader is referred to Laporte [51], Cohan [96] and Kara and Kurki-Suonio [43].

Because of the additional rotational axes between the pole and the equator on the unit sphere, the point groups T_h, O_h and Y_h require polyhedral (disdodecahedral, hexoctahedral and icosahedral) harmonics X_L which are linear combinations of S_l^m with fixed l and variable m. The whole family of X_L for the cubic crystal classes T, T_h, O, T_d and O_h is called "cubic harmonics" by Kurki-Suonio and coworkers [65, 66, 43], consistent with our nomenclature, while Fox and Krohn [97] restrict it so far to T_d (also "tetrahedral harmonics" [58]) and O_h, and Mueller and Priestley [98] even to O_h alone. Von der Lage and Bethe [70] use the term "kubic harmonics" for the lattice harmonics Λ_{kL} of the space group $O_h^9 = \mathrm{I}m\bar{3}m$ for $\boldsymbol{k} = 0$ and $\boldsymbol{k} = (\pi/a)\,\bar{\boldsymbol{e}}_z$. Since the point symmetry of these two $\boldsymbol{k}$-points is O_h, their X_L are hexoctahedral harmonics. The notation for the polyhedral harmonics has to be $X_{l,n}$ or X_L with the rules explained above.

The coefficients C_{lmL} of the disdodecahedral harmonics (T_h) can be taken from Kara and Kurki-Suonio ([43], Tab. 3 and 4) with their exact values for $l \leqq 10$, from Altmann and Cracknell ([74], Tab. I a, representation A_g) with 8 decimal digits for $l \leqq 12$, and with three more decimal digits from Bradley and Cracknell ([64], Table 2.6). The poly-

Table 3. Approximate locations of the maxima (+) and minima (−) of the hexoctahedral harmonics $L = 2$ to $L = 14$ ($l = 4$ to $l = 20$) on the first octant of the unit sphere. The first coordinate is the pole distance θ, the second the azimuthal angle φ, both in degrees. Each line contains the extrema which have the same distance to the [111]-direction and which are related by the symmetry elements located in [111].

$L = 2$	+	0 ; 0			90 ; 0			90 ; 90
$l = 4$	−				54.7; 45			
$n = 1$								
$L = 3$	+	0 ; 0			90 ; 0			90 ; 90
$l = 6$	−	45 ; 0			45 ; 90			90 ; 45
$n = 1$	+				54.7; 45			
$L = 4$	+	0 ; 0			90 ; 0			90 ; 90
$l = 8$	−	27.4; 45			71.0; 20.1			71.0; 69.8
$n = 1$	+	45 ; 0			45 ; 90			90 ; 45
	+				54.7; 45			
$L = 5$	+	0 ; 0			90 ; 0			90 ; 90
$l \doteq 10$	−	25 ; 0	25 ; 90	65 ; 0		65 ; 90	90 ; 25	90 ; 65
$n = 1$	+	33 ; 45			67.3; 24.7			67.3; 65
	−				54.7; 45			
$L = 6$	+	0 ; 0			90 ; 0			90 ; 90
$l = 12$	−	18.6; 45			77 ; 13.4			77 ; 76.6
$n = 1$	+	30.7; 0	30.7; 90	59.3; 0		59.3; 90	90 ; 30.7	90 ; 59.3
	+	35.8; 45			65.6; 27			65.6; 63
	−	46.7; 20.1			46.7; 69.9			75.5; 45
$L = 7$	+	24.1; 0	24.1; 90	65.9; 0		65.9; 90	90 ; 24.1	90 ; 65.9
$l = 12$	−	25.5; 45			72.2; 18.7			72.2; 71.3
$n = 2$	−	45 ; 0			45 ; 90			90 ; 45
	+	48.3; 23.7			46.9; 65.7			72.5; 45
	−				54.7; 45			
$L = 8$	+	0 ; 0			90 ; 0			90 ; 90
$l = 14$	−	16.3; 0	16.3; 90	73.7; 0		73.7; 90	90 ; 16.3	90 ; 73.7
$n = 1$	+	23.7; 45			73.5; 17.2			73.5; 72.8
	−	39.0; 45			63.6; 29.8			63.6; 60.2
	−	45 ; 0			45 ; 90			90 ; 45
	+				54.7; 45			
$L = 9$	+	0 ; 0			90 ; 0			90 ; 90
$l = 16$	−	13.9; 45			80.2; 9.9			80.2; 80.1
$n = 1$	+	23.2; 0	23.2; 90	66.8; 0		66.8; 90	90 ; 23.2	90 ; 66.8
	+	26.9; 45			71.3; 19.7			71.3; 70.3
	−	35.3; 19.5	35.3; 70.5	57 ; 13.3		57 ; 76.7	78.9; 33.7	78.9; 56.3
	+	45 ; 0			45 ; 90			90 ; 45
	+	48.4; 27.4			48.4; 62.6			69.9; 45
	−				54.7; 45			

hedral harmonics $X_{0,1}$, $X_{4,1}$, $X_{6,1}$, $X_{8,1}$, $X_{10,1}$, $X_{12,1}$, and $X_{12,2}$ are shared with the point group O_h in that range of l. We shall deal with the additional disdodecahedral harmonics $X_{6,2}$, $X_{10,2}$, $X_{12,3}$, etc. when required by our experiments.

V. The Hexoctahedral Harmonics

These are the polyhedral harmonics of the point group $O_h = m\bar{3}m$ which we have needed in the analysis of our Compton experiments on single-crystal lithium fluoride (Part III of the present series of papers). First given by von der Lage and Bethe [70] in cartesian form, they can be found as tables of the C_{lmL} in Ref. [43] (Tab. 3 and 4, exact values for $l \leqq 10$), Ref. [74] (Tab. 1 a, rep. A_{1g}, 8 decimal digits for $l \leqq 12$), Ref. [64] (Tab. 2.6, rep. A_{1g}, 11 decimal digits for $l \leqq 12$) and in Ref. [98] (Tab. 1, 8 decimal digits for $l \leqq 30$). A computer program owing to Fox and Krohn is available from the QCPE [97] which allows the computation of the C_{lmL} to 6 decimal digits for $l \leqq 100$.

Table 1. (continued)

$L = 10$	+	18.6; 0	18.6; 90	71.4; 0		71.4; 90	90 ; 18.6	90 ; 71.4
$l = 16$	−	19.5; 45			76.3; 14.1			76.3; 75.9
$n = 2$	−	34.4; 0	34.4; 90	56.6; 0		56.6; 90	90 ; 34.4	90 ; 56.6
	+	35 ; 30	35 ; 60	60.2; 19.3		60.2; 70.7	73.3; 31.2	73.3; 58.8
	+	45.7; 12.9			45.7; 77.1			80.8; 45
	−	48.9; 29.4			48.9; 60.6			68.3; 45
	+				54.7; 45			
$L = 11$	+	0; 0			90 ; 0			90 ; 90
$l = 18$	−	12.1; 0	12.1; 90	77.9; 0		77.9; 90	90 ; 12.1	90 ; 77.9
$n = 1$	+	19.5; 45			76.3; 14.1			76.3; 75.9
	−	30.7; 45			68.8; 22.8			68.8; 67.2
	−	34.4; 0	34.4; 90	55.6; 0		55.6; 90	90 ; 34.4	90 ; 55.6
	+	42.7; 45			61.3; 33.1			61.3; 56.9
	+	45.7; 12.5			45.7; 77.5			81.1; 45
	−	48.8; 28.5			48.8; 61.5			69 ; 45
$L = 12$	−	29.7; 0	29.7; 90	60.3; 0		60.3; 90	90 ; 29.7	90 ; 60.3
$l = 18$	+	31.6; 24.5	31.6; 65.6	61.5; 14.3		61.5; 75.7	77.5; 29.2	77.5; 60.8
$n = 2$	−	33.4; 45			67.1; 25			67.1; 65
	+	45 ; 0			45 ; 90			90 ; 45
	−	46.4; 16.8			46.4; 73.2			77.9; 45
	+	49.5; 31.3			49.5; 58.7			66.7; 45
	−				54.7; 45			
$L = 13$	+	0 ; 0			90 ; 0			90 ; 90
$l = 20$	−	11.1; 45			82.2; 7.9			82.2; 82.1
$n = 1$	+	18.7; 0	18.7; 90	71.3; 0		71.3; 90	90 ; 18.7	90 ; 71.3
	+	21.5; 45			75 ; 15.6			75 ; 74.4
	−	28.4; 19	28.4; 71	63.3; 10		63.3; 80	81.1; 27.1	81.1; 62.9
	+	36.2; 0	36.2; 90	53.8; 0		53.8; 90	90 ; 36.2	90 ; 53.8
	+	43.2; 45			61.6; 33.6			61.6; 56.4
	−	45.7; 12.7			45.7; 77.3			80.9; 45
	+				54.7; 45			
$L = 14$	+	14.8; 0	14.8; 90	75.2; 0		75.2; 90	90 ; 14.8	90 ; 75.2
$l = 20$	−	15 ; 45			79.5; 10.7			79.5; 79.3
$n = 2$	−	25.9; 0	25.9; 90	64.1; 0		64.1; 90	90 ; 25.9	90 ; 64.1
	+	26.2; 45			71.8; 19.2			71.8; 70.8
	+	36.5; 12.5	36.5; 77.5	54.5; 9.1		54.5; 80.9	82.6; 35.8	82.6; 54.2
	−	36.5; 31.5	36.5; 58.5	59.5; 21.1		59.5; 68.9	71.9; 32.3	71.9; 57.7
	+	43.7; 45			60.7; 34.1			60.7; 55.9
	−	45 ; 0			45 ; 90			90 ; 45
	−				54.7; 45			

The selection rule for l and n of the $X_{l,n}$ can be determined from a table for the point group O by Bethe [52] and Döring [63] and the fact that the additional inversion centre in the point group O_h eliminates all odd l. If k is a non-negative integer number, then there are $k+1$ different n for $l = 12k$, k for $l = 12k+2$, and $k+1$ for $l = 12k+4$, $l = 12k+6$, $l = 12k+8$ and $l = 12k+10$ each. The resulting sequence of l with increasing L is 0, 4, 6, 8, 10, 12, 12, 14, 16, 16, 18, 18, 20, 20, 22, 22, 24, 24, 24, 26, 26, 28, 28, 28, 30, 30, 30, 32, 32, 32, 34, 34, 34, 36, 36, 36, 36, 38, 38, 38, 40, 40, 40, 40, etc.

Difficulties arose during our analysis of the experimental data because of the serious lack of published information concerning the behaviour of the hexoctahedral harmonics on the unit sphere. Such information is important in order to judge whether and to which degree a measurement influences the contribution of a certain X_L, and to predict the interpolation behaviour of a particular X_L regarding, for example, oscillations which are not sufficiently limited by the experimental data. Already when planning the experiments one should take the angular dependence of the various X_L into account, as will be shown in the forthcoming Part II.

For these reasons we display the first 13 aspherical hexoctahedral harmonics ($l \leqq 20$) as polar contour diagrams (based on a 55×55 point mesh, contour determination with a computer program owing to P. Bischof) in Figure 1 a–m. In addition we have determined the location of the extrema in the first octant and collected the angular coordinates in Table 3, ordered by equivalence under the symmetry operations which are centred in the [111]-point on the unit sphere. From Fig. 1 and Table 3 it can be seen, for example, that $X_2 = X_{4,1}$ mainly describes the difference between the $\langle 100 \rangle$ and $\langle 111 \rangle$-directions, and that $X_3 = X_{6,1}$ is then dominated by the $\langle 110 \rangle$-directions, while $X_4 = X_{8,1}$ is determined by the $\langle 311 \rangle$ and $X_5 = X_{10,1}$ by the $\langle 210 \rangle$-directions. Because of the higher amplitudes with increasing l we had to coarsen the contour scale from $L = 7$, and for $L = 13$ and 14 the θ-scale had to be enlarged in order to resolve the finer structure with the given mesh of points.

Acknowledgements

This work is devoted with sincere gratitude to our teacher for many years, Prof. Dr. Alarich Weiss, on occasion of his sixtieth birthday. Particularly for one of us (W. W.) he has been much more than just a Doktorvater.

We would further like to express our thanks to the Deutsche Forschungsgemeinschaft and to the Fonds der Chemischen Industrie for their financial support.

[1] B. Williams (ed.), Compton Scattering. The Investigation of Electron Momentum Distributions, McGraw-Hill, New York 1977.
[2] W. Weyrich, Einige Beiträge zur Compton-Spektroskopie, Habilitationsschrift, Darmstadt 1978.
[3] B. G. Williams and J. M. Thomas, Intern. Rev. Phys. Chem. **3,** 39 (1983).
[4] M. J. Cooper, Rep. Progr. Phys., in print.
[5] J. W. M. DuMond, Rev. Mod. Phys. **5,** 1 (1933).
[6] S. Chandrasekhar, Ellipsoidal Figures of Equilibrium, Yale University Press, New Haven 1969.
[7] L. Cohen, J. Math. Phys. **19,** 1838 (1978).
[8] W. Weyrich, Ber. Bunsenges. Phys. Chem. **83,** 797 (1979).
[9] A. M. Nyanda and B. G. Williams, Phil. Mag. **B40,** 97 (1979).
[10] P. E. Mijnarends, Phys. Rev. **160,** 512 (1967).
[11] P. E. Mijnarends, Positron annihilation in metals. A contribution to the analysis of angular correlation measurements with an application to copper, Ph.D. Thesis, Technische Hogeschool, Delft 1969.
[12] P. E. Mijnarends, Unfold. A Fortran-IV code for the synthesis of momentum distributions by deconvolution of angular correlations of positron annihilation radiation or Compton line profiles, **Vol. I** and **II,** RCN Report 217, Reactor Centrum Nederland, Petten 1974.
[13] P. E. Mijnarends, Phys. Rev. **178,** 622 (1969).
[14] P. E. Mijnarends, Physica **63,** 248 (1973).
[15] P. E. Mijnarends, Appl. Phys. **4,** 303 (1974).
[16] P. E. Mijnarends, Phys. Rev. **B4,** 2820 (1971).
[17] W. Schülke, Phys. Stat. Sol. (b) **62,** 453 (1974).
[18] C. K. Majumdar, Phys. Rev. **B4,** 2111 (1971).
[19] F. M. Mueller, Bull. Amer. Phys. Soc. II, **19,** 200 (1974).
[20] F. M. Mueller, Phys. Rev. **B15,** 3039 (1977).
[21] W. A. Reed, unpublished (1974).
[22] P. Pattison, W. Weyrich, and B. G. Williams, Sagamore V Conference, Kiljava, Finland 1976.
[23] N. K. Hansen, Reconstruction of the Electron Momentum Distribution from a Set of Directional Compton Profiles, Report HMI-B **342,** Hahn-Meitner-Institut, Berlin 1980.
[24] P. Pattison, N. K. Hansen, and J. R. Schneider, Chem. Phys. **59,** 231 (1981).
[25] H. Heuser, Reziproker Formfaktor und Impulsdichte der Elektronen in kristallinem Lithiumhydroxid, Dissertation, Darmstadt 1981.
[26] E. Heuser and W. Weyrich, Conference on X-Ray and Electron Scattering for the Determination of Electronic Structures, Metz 1981; Fourth International Congress in Quantum Chemistry, Uppsala 1982; Sanibel Symposia, Part I, Palm Coast (Florida) 1984. XIIIth International Congress and General Assembly, International Union of Crystallographic, Hamburg 1984, and Acta Cryst. **40,** Suppl., C-171 (1984).
[27] E. Heuser, Erhöhung der Genauigkeit von Compton-Profilen: Optimierung der Streugeometrie, Eliminierung der Mehrfachstreuung und das Compton-Profil von Wasser, Diplomarbeit, Darmstadt 1976.
[28] E. Heuser and W. Weyrich, Jül-Conf-22, Kernforschungsanlage Jülich, 1976.
[29] S. Manninen and T. Paakkari, Nucl. Inst. Meth. **155,** 115 (1978).
[30] M. J. Cooper, R. S. Holt, and J. L. DuBard, J. Phys. **E11,** 1145 (1978).
[31] W. Weyrich, Sagamore VI Conference, Mont Tremblant, Canada 1979.
[32] P. Bachmann, Compton-spektroskopische Untersuchung organischer Moleküle, Dissertation, Darmstadt 1979.
[33] P. Pattison and J. R. Schneider, Nucl. Instr. Meth. **158,** 145 (1979).
[34] R. S. Holt, M. Copper, J. L. DuBard, J. B. Forsyth, T. L. Jones, and K. Knights, J. Phys. **E12,** 1148 (1979).
[35] P. Pattison and W. Weyrich, XIIIth International Congress and General Assembly, International Union of Crystallography, Hamburg 1984, and Acta Cryst. **40,** Suppl., C-157 (1984).
[36] E. W. Hobson, The Theory of Spherical and Ellipsoidal Harmonics, Cambridge University Press, Cambridge 1931 (reprint: Chelsea Publishing Company, 2nd printing, New York 1965).
[37] W. Magnus, F. Oberhettinger, and R. P. Soni, Formulas and Theorems for the Special Functions of Mathematical Physics, Die Grundlehren der mathematischen Wissenschaften in Einzeldarstellungen, Band 52, 3rd edition, Springer-Verlag, Berlin 1966.
[38] M. Abramowitz and I. A. Stegun (eds.), Handbook of Mathematical Functions, 7th printing, Dover Publications, Inc., New York (after 1970).
[39] I. S. Gradshteyn and I. M. Ryzhik, Table of Integrals, Series and Products, 4th ed., 7th printing, Academic Press, New York 1973.

[40] M. E. Rose, Elementary Theory of Angular Momentum, 5th printing, John Wiley & Sons, Inc., New York 1967.

[41] A. Messiah, Quantum Mechanics, 3rd printing, North-Holland Publishing Company, Amsterdam 1965.

[42] B. Spain and M. G. Smith, Functions of Mathematical Physics, Van Nostrand Reinhold Company, New York 1970.

[43] M. Kara and K. Kurki-Suonio, Acta Cryst. **A37,** 201 (1981).

[44] G. A. Korn and T. M. Korn, Mathematical Handbook for Scientists and Engineers, 2nd ed., McGraw-Hill, New York 1968.

[45] I. N. Sneddon, Special Functions of Mathematical Physics and Chemistry, 3rd ed., Longman Group Ltd., London 1980.

[46] F. Klein, Vorlesungen über das Ikosaeder, Leipzig 1884.

[47] E. Goursat, Ann. École Norm. Sup. (3) **4,** 158 (1887).

[48] E. Pockels, Über die Differentialgleichung $\Delta u + k^2 u = 0$, Leipzig 1891.

[49] E. G. C. Poole, Proc. London Math. Soc. (2) **33,** 435 (1932).

[50] J. Hodgkinson, J. London Math. Soc. **10,** 221 (1935).

[51] O. Laporte, Z. Naturforsch. **3a,** 447 (1948).

[52] H. Bethe, Ann. Physik (5) **3,** 133 (1929).

[53] W. Ehlert, Z. Physik **51,** 6 (1928).

[54] H. A. Jahn, Proc. Roy. Soc., London **A168,** 469 (1938).

[55] H. A. Jahn, Proc. Roy. Soc., London **A168,** 495 (1938).

[56] K. T. Hecht, J. Mol. Spectrosc. **5,** 355 (1960).

[57] J. Moret-Bailly, J. Mol. Spectrosc. **15,** 344 (1965).

[58] K. Fox and I. Ozier, J. Chem. Phys. **52,** 5044 (1970).

[59] B. Meyer, Can. J. Math. **6,** 135 (1954).

[60] M. A. Melvin, Rev. Mod. Phys. **28,** 18 (1956).

[61] S. L. Altmann, Proc. Camb. Phil. Soc. **53,** 343 (1957).

[62] S. L. Altmann, Phil. Trans. Roy. Soc., London **A255,** 199 (1963).

[63] W. Döring, Ann. Physik (7) **1,** 102 (1958).

[64] C. J. Bradley and A. P. Cracknell, The Mathematical Theory of Symmetry in Solids, Clarendon Press, Oxford 1972.

[65] K. Kurki-Suonio, Isr. J. Chem. **16,** 115 (1977).

[66] K. Kurki-Suonio, I. Merisalo, and H. Peltonen, Phys. Scripta **19,** 57 (1979).

[67] International Tables for Crystallography, **Vol. A,** Space-Group Symmetry (ed. by Th. Hahn), D. Reidel Publ. Company, Dordrecht 1983.

[68] E. P. Wigner and F. Seitz, Phys. Rev. **46,** 509 (1934).

[69] L. P. Bouckaert, R. Smoluchowski, and E. Wigner, Phys. Rev. **50,** 58 (1936).

[70] F. C. von der Lage and H. A. Bethe, Phys. Rev. **71,** 612 (1947).

[71] D. J. Howarth and H. Jones, Proc. Phys. Soc., London **A65,** 355 (1952).

[72] D. G. Bell, Rev. Mod. Phys. **26,** 311 (1954).

[73] S. L. Altmann, Proc. Roy. Soc., London **244,** 141 (1958).

[74] S. L. Altmann and A. P. Cracknell, Rev. Mod. Phys. **37,** 19 (1965).

[75] S. L. Altmann and C. J. Bradley, Rev. Mod. Phys. **37,** 33 (1965).

[76] C. Herring, J. Franklin Inst. **233,** 525 (1942).

[77] M. Atoji, Acta Cryst. **11,** 827 (1958).

[78] R. J. Weiss, Phys. Letters **12,** 293 (1964).

[79] J. J. DeMarco and R. J. Weiss, Phys. Rev. (A) **137,** 1869 (1965).

[80] B. Dawson, Austral. J. Chem. **18,** 595 (1965).

[81] B. Dawson, Proc. Roy. Soc., London **A298,** 255, 264, 379, 395 (1967).

[82] B. Dawson and P. L. Sanger, Proc. Roy. Soc., London **A301,** 195 (1967).

[83] K. Kurki-Suonio and V. Meisalo, Ann. Acad. Sci. Fennicae **AVI, 241,** 1 (1967).

[84] K. Kurki-Suonio, Ann. Acad. Sci. Fennicae **AVI, 263,** 3 (1967).

[85] R. F. Stewart, J. Chem. Phys. **51,** 4569 (1969).

[86] R. F. Stewart, J. Chem. Phys. **57,** 1664 (1972).

[87] R. F. Stewart, J. Chem. Phys. **58,** 1668, 4430 (1973).

[88] R. F. Stewart, J. Chem. Phys. **63,** 3031 (1975).

[89] R. F. Stewart, Acta Cryst. **A32,** 565 (1976).

[90] R. F. Stewart, Isr. J. Chem. **16,** 114 (1977).

[91] F. L. Hirshfeld, Acta Cryst. **B27,** 769 (1971).

[92] M. Harel and F. L. Hirshfeld, Acta Cryst. **B31,** 162 (1975).

[93] F. L. Hirshfeld, Acta Cryst. **A32,** 239 (1976).

[94] P. O. Löwdin, Adv. Quantum Chem. **3,** 339 (1967).

[95] A. J. Thakkar, A. M. Simas, and V. H. Smith, Jr., J. Chem. Phys. **81,** 2953 (1984).

[96] N. V. Cohan, Proc. Camb. Phil. Soc. **54,** 28 (1958).

[97] K. Fox and B. J. Krohn, J. Comput. Phys. **25,** 386 (1977), and Program No. 347, Quantum Chemistry Program Exchange, Department of Chemistry, Indiana University, Bloomington, Indiana 47401, USA.

[98] F. M. Mueller and M. G. Priestley, Phys. Rev. **148,** 638 (1966).